A precursor form of vascular endothelial growth factor arises by initiation from an upstream in-frame CUG codon

Meng Kian TEE[1] and Robert B. JAFFE

Center for Reproductive Sciences, University of California, San Francisco, San Francisco, CA 94143-0556, U.S.A.

Vascular endothelial growth factor (VEGF) is a mitogen in physiological and pathological angiogenesis. Understanding the expression of different VEGF isoforms might be important for distinguishing angiogenesis in tissue development, vascular remodelling and tumour formation. We examined its expression and noted the presence of the isoforms $VEGF_{121}$ and $VEGF_{165}$ (121 and 165 residues long respectively) in fetal heart, lung, ovary, spleen, placenta and ovarian tumours. Unexpectedly, a 47 kDa species predominated in fetal intestine and muscle. The presumed initiation site in VEGF is an AUG codon (AUG^{1039}), 1039 nt from its main transcriptional start site. AUG^{1039} is preceded in the 5′ untranslated region by an in-frame CUG at nt 499 (CUG^{499}), which could produce the 47 kDa form with a 180-residue N-terminal extension. We therefore assessed whether CUG^{499} functions as an initiator. CUG^{499} initiation produced the 47 kDa $VEGF_{165}$ precursor, which was processed at two sites to yield VEGF and three N-terminal fragments. When CTG^{499} was mutated to CGC, the precursor and N-terminal fragments were barely detectable. Although the precursor form was predominant in $VEGF_{165}$, both CUG^{499} and AUG^{1039} forms were found in $VEGF_{121}$. VEGF precursor induced neither the proliferation of human umbilical vein endothelial cells nor the expression of angiopoietin 2, which can be induced by, and act with, VEGF to induce tumour angiogenesis. The precursor also adheres to the extracellular matrix (ECM), suggesting that it might be a storage form for generating active VEGF in the cell or ECM. Alternate CUG^{499} and AUG^{1039} initiation and processing of the inactive precursor and its products might be important in regulating angiogenesis.

Key words: angiogenesis, proteolysis, translation initiation.

INTRODUCTION

Vascular endothelial growth factor (VEGF), also known as vascular permeability factor, is an endothelium-specific mitogen that is pivotal in physiological and pathological angiogenesis. VEGF biological activities include the stimulation of endothelial cell growth and migration, the enhancement of microvascular permeability *in vivo*, the promotion of vasculogenesis and angiogenesis and the induction of embryonic stem cell differentiation into haemopoietic precursors [1].

The human VEGF gene is approx. 14 kb long, containing eight exons that give rise to a full-length mature polypeptide of 206 residues. Isoforms of 121, 145, 165 and 189 residues exist owing to alternative splicing. Except for $VEGF_{145}$, the mouse homologues are $VEGF_{120}$, $VEGF_{164}$ and $VEGF_{188}$. The common isoforms, $VEGF_{121}$ and $VEGF_{165}$, contain exons 1–5 and 8, and 1–5 and 7–8 respectively. $VEGF_{165}$, a 45 kDa homodimeric, heparin-binding glycoprotein, is a secreted product, although a significant portion is cell-associated. $VEGF_{121}$ is weakly acidic and secreted. Both isoforms show a dose-dependent mitogenic effect on endothelial cells. However, the lack of heparin-binding in $VEGF_{121}$ leads to a significant loss of mitogenic activity in comparison with $VEGF_{165}$ [1–4]. Mice expressing $VEGF_{120}$ but lacking $VEGF_{164}$ and $VEGF_{188}$ have impaired myocardial angiogenesis, which leads to ischaemic cardiomyopathy [5].

Translation of the VEGF mRNA is assumed to be initiated at an AUG codon (AUG^{1039}), which is 1039 nt from its major transcriptional start site [6,7]. The flanking sequences ACC AUG A contain Kozak's consensus sequence $^{A}_{G}$CC AUG G [8] and the first 26 residues of the predicted AUG^{1039} product resemble a signal peptide. Cleavage of the 26 residues from the AUG^{1039} product is assumed to yield mature VEGF, with alanine as the first residue.

An alternate transcriptional start site of VEGF is present 633 nt downstream of the major site [9]. An internal ribosome entry site (IRES), which allows a cap-independent mode of initiation, is approx. 300 nt upstream of AUG^{1039}. This IRES (IRES A) contains at least two elements; another IRES is between nt 91 and 483 (IRES B) [9–12].

An in-frame CUG codon at nt 499 (CUG^{499}) in the 5′ VEGF untranslated region (UTR) [3] might also function as an initiator and could produce a larger form of VEGF with 180 residues in the N-terminus, extended from the Met of AUG^{1039}. CUG^{499}-flanking sequences GCG CUG^{499} A are conserved in cow [7], rat [13] and mouse [14]. The multiple putative transcriptional initiation sites in the 5′ UTR indicate that tissues might produce multiple VEGF isoforms depending on their degree of differentiation or angiogenesis. We have been interested in determining whether the VEGF isoforms expressed in normal tissues are the same as those expressed in tumours, because the different isoforms seem to exhibit distinct biological properties. Understanding the expression of different VEGF isoforms might be important for distinguishing between angiogenesis that occurs during tissue development, vascular remodelling and tumour formation. In the present study we investigated the VEGF isoforms expressed in normal human fetal tissues and ovarian tumours. We found that ovarian tumours and some fetal tissues express a 47 kDa VEGF precursor protein, which arises predominantly from CUG^{499} initiation. The VEGF precursor, which can interact with the extracellular matrix (ECM), also undergoes

Abbreviations used: Ang2, angiopoietin 2; CM, conditioned medium; ECM, extracellular matrix; FLAG, Asp-Tyr-Lys-Asp-Asp-Asp-Asp-Lys; HUVEC, human umbilical-vein endothelial cells; IRES, internal ribosome entry site; mAUG, mutant AUG^{1039}; mCUG, mutant CUG^{499}; PDGF, platelet-derived growth factor; UTR, untranslated region; VE-cadherin, vascular endothelial cadherin; VEGF, vascular endothelial growth factor; wt, wild-type.

[1] To whom correspondence should be addressed (e-mail mktee@itsa.ucsf.edu).

proteolysis at two sites to produce VEGF and 10, 22 and 28 kDa N-terminal fragments. These studies suggest that the precursor is processed into active VEGF isoforms, which participate in angiogenesis in tumour tissues.

EXPERIMENTAL

DNA constructs

All PCR was done with *Pfu* DNA polymerase (Stratagene, La Jolla, CA, U.S.A.), and all cDNA species were sequenced in their entirety on both strands of DNA with standard vector primers and internal primers with an ABI automated sequencer at the University of California, San Francisco (UCSF) Biomolecular Resource Center (San Francisco, CA, U.S.A.).

To clone full-length $VEGF_{121}$ and $VEGF_{165}$ cDNA species, cytoplasmic RNA of the SKOV3 ovarian cancer cell line was reverse-transcribed with random primers and amplified with primers 5′-TATTATAAGCTTTCGCGGAGGCTTGGGGCAG-3′ (sense) and 5′-GATATACTCGAGTCTAGATCACCGCCTCGGCTTGTCACA-3′ (anti-sense). The PCR products were cloned into pCMV vector. Sequences of the full-length VEGF cDNA species agreed with the published sequence [3]. To delete the first 956 nt of the 5′ UTR in 165 Δ956, $VEGF_{165}$ cDNA was digested with *Nar*I/*Hin*dIII and Klenow-treated with all four dNTPs (50 μM); the linearized plasmid DNA was then religated.

Site-directed mutagenesis was performed with the QuikChange Site-Directed Mutagenesis kit (Stratagene). Full-length mutant CUG (mCUG) has codon CGC (Arg) replacing CTG^{499} (Leu^{1}); this was done with $VEGF_{121}$ and $VEGF_{165}$ wild-type (wt) templates by using primers 5′-CTGACCAGTCGCGCGCACGGACAGAC-3′ (sense) and 5′-GTCTGTCCGTGCGCGCGACTGGTCAG-3′ (anti-sense). Mutation of ATG^{1039} to GTC (Val) in mutant AUG (mAUG) was done with primers 5′-CGGGCCTCCGAAACCGTCAACTTTCTGCTG-3′ (sense) and 5′-CAGCAGAAAGTTGACGGTTTCGGAGGCCCG-3′ (anti-sense). *Bss*HII and *Hin*cII sites respectively were created by these mutations, facilitating the screening of bacterial colonies. Double mutants of CUG^{499} and AUG^{1039} were made by ligating a 588 nt *Hin*dIII–*Sac*II fragment from the mCUG plasmid to *Hin*dIII/*Sac*II-digested mAUG vectors.

To make constructs F-Sac, which had the Asp-Tyr-Lys-Asp-Asp-Asp-Asp-Lys (FLAG) tag via site *Sac*II, between Arg^{30} and Gly^{31} in VEGF precursor, VEGF cDNA species were digested with *Sac*II, Klenow-treated with 50 μM dGTP and ligated to preannealed oligonucleotides 5′-CCGCGACTACAAGGACGACGACGACAAG-3′ (sense) and 5′-CCCCTTGTCGTCGTCGTCCTTGTAGTCGC-3′ (anti-sense). Constructs F-Nar had the FLAG tag via site *Nar*I, between Gly^{153} and Ala^{154}, and were made by digesting VEGF cDNA species with *Nar*I, Klenow treatment with dCTP and ligation to preannealed oligonucleotides 5′-GAGGCGGATCCGACTACAAGGACGACGACGACAAGCG-3′ (sense) and 5′-GGCGCGCTTGTCGTCGTCGTCCTTGTAGTCGGATC-3′ (anti-sense). To make constructs F-Mut, in which 10 residues in proteolytic site 1 were replaced by the FLAG epitope, PCR was performed with primers 5′-CATTATAAGCTTTCGCGGAGGCTTGGGGCAG-3′ (sense) and 5′-GTCCTTGTAGTCGACGTAGAGCAGCAAGGCGAG-3′ (anti-sense). The PCR product was Klenow-treated with dGTP and digested with *Hin*dIII. PCR also was performed with primers 5′-ACGACGATGACAAGCTTCCCATGGCAGAAGGAGGA-3′ (sense) and 5′-GATATACTCGAGTCTAGATCACCGCCTCGGCTTGTCACA-3′ (anti-sense); the PCR product was Klenow-treated in dCTP and digested with *Xba*I. Both PCR products were cloned into pCMV vector. Constructs F-Sac-Mut had the *Sac*II FLAG tag plus the 10-residue mutation/tag of proteolytic site 1; they were made by removing a 695 nt *Nhe*I fragment from the F-Mut plasmids and ligation of a 695 nt *Nhe*I fragment from the F-Sac plasmids.

To delete the first 475 nt (*Bam*HI) and 485 nt (*Pvu*II) of the 5′ UTR, F-Sac-Mut plasmids were digested with *Bam*HI and with *Pvu*II/*Xba*I respectively. The *Bam*HI-digested plasmids were Klenow-treated, digested with *Xba*I and cloned into pCMV vector (digested with *Hin*dIII, Klenow-treated and digested with *Xba*I). To delete sequences between sites *Sac*II and *Sma*I (nt 588 and 919), F-Mut plasmids were digested with *Sac*II, Klenow-treated and digested with *Xba*I. These vectors were ligated to *Sma*I/*Xba*I fragments from F-Mut plasmids. To delete sequences between sites *Xmn*I and *Sma*I (nt 658 and 919), F-Sac-Mut plasmids were digested with *Hin*dIII and *Xmn*I, and with *Sma*I and *Xba*I, to yield respectively 663 nt, and 564 and 696 nt fragments, and cloned into pCMV vector.

The DNA sequence encoding proteolytic site 2 is upstream of site *Nar*I. Thus, to make construct N-terminal-22k, which produced a product analogous to the 22 kDa N-terminal fragment, $VEGF_{165}$ cDNA was digested with *Nar*I/*Xba*I. A TAG stop codon was introduced downstream of site *Nar*I by ligating the digested plasmid to preannealed oligonucleotides 5′-CGCTAGGCCGAGGAGAGCGGGCGG-3′ (sense) and 5′-CTAGCGGCCCGCTCTCCTCGGCCTAG-3′ (anti-sense).

Tissue samples

Human fetal tissues were obtained from second-trimester pregnancies (16–23 weeks) after elective termination. Gestational age was estimated by foot length. Ovarian tumours were obtained from the ovarian cancer tissue bank courtesy of Dr K. Smith-McCune (UCSF Cancer Center, San Francisco, CA, U.S.A.).

Cell culture

COS-1 and SKOV3 were grown in Dulbecco's modified Eagle's medium H21, and OVCAR3 in RPMI-1640. These cell lines were obtained from A.T.C.C. (Manassas, VA, U.S.A.). Human umbilical-vein endothelial cells (HUVEC) were purchased from Clonetics (San Diego, CA, U.S.A.) and cultured in EGM medium.

Transfection

Transfection was done with the Effectene reagent (Qiagen, Valencia, CA, U.S.A.). To monitor transfection efficiency, a pGL3-luc control plasmid was included in each transfection. Transfection time was 24–48 h depending on cell type. Before being harvested, cells were incubated in conditioned medium (CM) for 24 h.

Cell proliferation assay

Subconfluent HUVEC (six-well plates, passage 4–5) were transfected with 165 Δ956 and 165 F-Sac-Mut mAUG, grown for 48 h, trypsinized, replated at lower densities and grown for a further 48 h. The cell proliferation assay was performed in triplicate from three separate transfection experiments with a Celltiter 96 aqueous one-solution cell proliferation assay from Promega (Madison, WI, U.S.A.). D_{490} data were normalized to transfection efficiency.

Monolayer and ECM preparation

Cells were incubated with 125 mM NaCl/5 mM KCl/50 mM Hepps (pH 7)/5 mM glucose/1 mM EDTA (pH 8) at 37 °C for

10 min and washed twice in the same buffer [15]. The monolayer was collected and pelleted, then lysed in the presence of protease inhibitors. The ECM portion was washed with PBS, pelleted and lysed. The ECM protein content was 2% of the cell monolayers, as determined with the protein assay kit (Bio-Rad, Hercules, CA, U.S.A.).

Western blotting

For Western blotting, proteins were transferred to a PVDF membrane (Millipore, Bedford, MA, U.S.A.). The antibodies used were against human VEGF (Upstate Biotech, Lake Placid, NY, U.S.A.), M2 FLAG (Sigma, St Louis, MO, U.S.A.), vascular endothelial cadherin (VE-cadherin; Research Diagnostics, Flanders, NJ, U.S.A.), angiopoietin 2 (Ang2; a gift from Dr G. D. Yancopoulos, Regeneron, Tarrytown, NY, U.S.A.) and the unique 180 N-terminal residues (described below). An ECL® Plus enhanced chemiluminescence detection system (Amersham, Arlington Heights, IL, U.S.A.) was used.

N-terminal antibody

To express the 180-residue N-terminal fragment in *Escherichia coli*, PCR was performed with primers 5′-AAAGGATCCCT-GACGGACAGACAGACAGAC-3′ (sense) and 5′-AAAGAA-TTCGGTTTCGGAGGCCCGACC-3′ (anti-sense). The PCR product was cloned into pET-21a vector (Novagen, Madison, WI, U.S.A.). Purification of the 180-residue peptide with the His-bind resin was done as recommended by the manufacturer. The polyclonal antibody was produced in rabbits by using the BabCO (Richmond, CA, U.S.A.) custom antibody service. The specificity of the T7N4 antibody was tested with the purified N-terminal peptide.

RESULTS

Endogenous expression of a 47 kDa VEGF form

We initially sought to determine VEGF expression in ovarian tumours and fetal tissues using Western blotting with anti-VEGF antibody. We observed 15, 18 and 23 kDa bands (Figure 1A, lanes 1–6, 10 and 11), corresponding to the sizes of $VEGF_{121}$ and $VEGF_{165}$ respectively [2]. Unexpectedly, all ovarian tumours (Figure 1A, lanes 2–4) and most of the fetal tissues studied (lanes 5 and 8–11) produced a 47 kDa band, which could have been a large VEGF form with a 180-residue N-terminal extension, initiated from CUG^{499}. The 30 kDa band in Figure 1(A), lanes 1–7 and 9–11, could have been non-specific because we also observed this pattern in the transfection experiments described below. To explore the expression and role of the 47 kDa band, we raised T7N4 antibody against the 180 N-terminal residues (Figure 1B) and analysed a fetal ovary and four ovarian tumours by Western blotting. The 47 kDa band previously detected with anti-VEGF antibody was detected in the same ovarian tumours with antibody T7N4 (Figure 1C). Because the CUG^{499} product contained proteolytic site 1, this cleavage alone was likely to yield VEGF and an N-terminal fragment (Figure 1B). However, antibody T7N4 also recognized 28 and 22 kDa bands (Figure 1C), which were probably N-terminal fragments arising from proteolysis of the precursor.

Product from CUG^{499}, the predominant upstream initiator, undergoes proteolysis

To determine whether the 47 kDa band originated from CUG^{499} initiation, full-length cDNA species were tagged with FLAG;

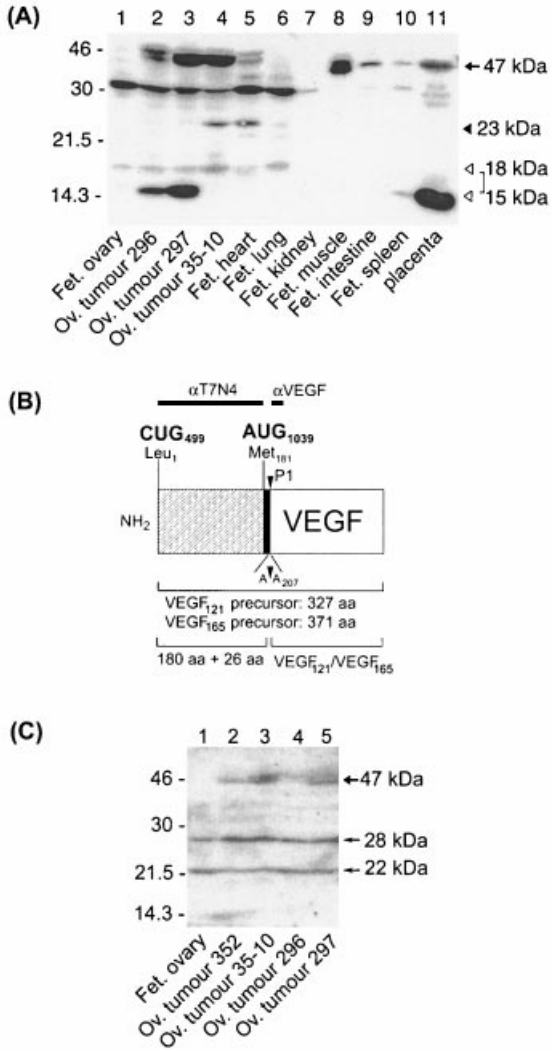

Figure 1 Expression of a 47 kDa form of VEGF

(**A**) Western blotting of tissues from the human fetus and ovarian tumours, analysed under reducing conditions with anti-VEGF antibody, raised against the first 20 residues of mature VEGF. VEGF contains a single N-linked glycosylation site at Asn^{281}, relative to Leu^{1} of CUG^{499}. $VEGF_{121}$ and $VEGF_{165}$ migrate as doublets of 15/18 and 21/23 kDa under reducing conditions, probably as unglycosylated/glycosylated forms [2]. The 30 kDa band, which showed intensity variations in different tissues, might be a background band. (**B**) Schematic representation of VEGF precursor. Because the sequence of VEGF begins at Ala^{207} [4], a cleavage (downwards-pointing arrow) probably occurs between Ala^{206} and Ala^{207}, hereafter referred to as proteolytic site 1 (P1). The sequence of the 26 residues (aa) between Met^{181} and P1 (black box) resemble that of a signal peptide [6,7]. The unique N-terminal portion (grey box) is between Leu^{1} and Met^{181}. Because the predicted CUG^{499} and AUG^{1039} products contain P1, VEGF could be derived from the proteolysis of either protein. (**C**) Western blotting of four ovarian tumours and a fetal ovary sample, probed under reducing conditions with antibody T7N4. The additional 22 and 28 kDa bands present in these samples could be proteolytic products of the 47 kDa band. Results are representative of three separate experiments. The positions of molecular mass markers are indicated (in kDa) at the left in (**A**) and (**C**).

mutations of CTG^{499} to CGC and ATG_{1039} to GTC were introduced into a subset of these constructs (Figure 2A). Whereas the mutational analysis permitted the evaluation of whether CUG^{499} was used for initiation, the introduction of tags at sites *Sac*II and *Nar*I permitted the detection of this initiation product and also a determination of the origins of the 28 and 22 kDa fragments seen in Figure 1(C). After transfection into COS1

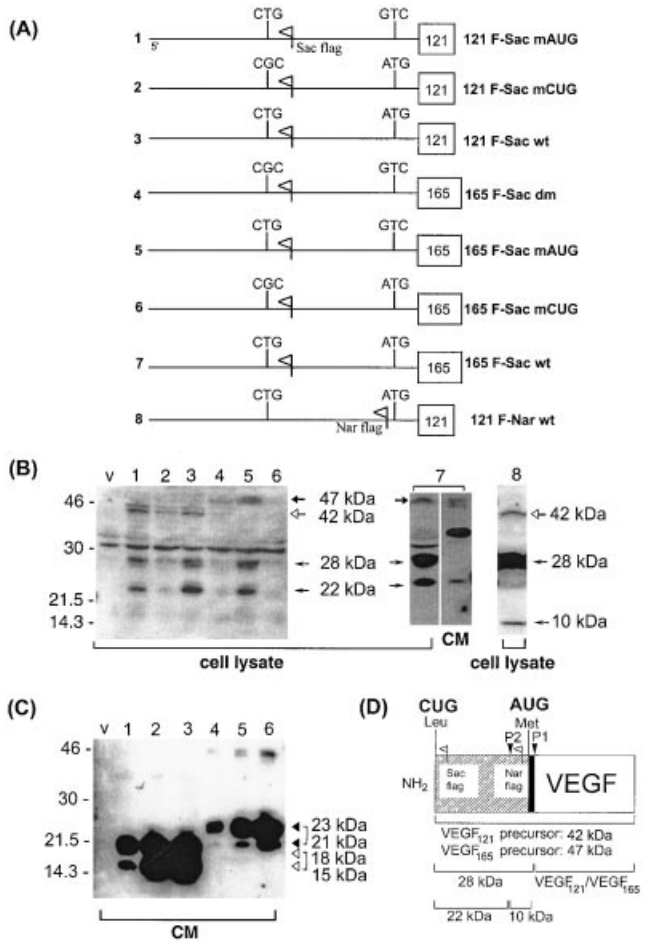

Figure 2 CUG^{499} precursor is processed at two sites

(**A**) Line drawing of epitope-tagged VEGF$_{121}$ and VEGF$_{165}$. The FLAG tag was between either Arg^{30} and Gly^{31} (Sac flag) or Gly^{153} and Ala^{154} (Nar flag), carboxy-terminal to the Leu^{1} of CUG^{499}. Abbreviation: dm, double mutant CUG^{499} + AUG^{1039}. (**B**) The above constructs were transfected into COS1 cells and the Western blot was probed with anti-FLAG antibody under reducing conditions. The lane numbers correspond to the construct numbers above; lane v represents transfection with the vector alone. The 30 kDa band might be non-specific because it was also present in the vector lane. Similarly, the 35 kDa band in CM (lane 7) could also be non-specific because it was detected in vector alone (results not shown). (**C**) Western blot of the above samples, probed with anti-VEGF antibody under reducing conditions. Although the weak 46 kDa band in lanes 4–6 has a size comparable to the VEGF$_{165}$ precursor, it can also arise by aggregation or incomplete reduction when VEGF$_{165}$ dimers are present at high concentration. (**D**) Summary of VEGF precursor proteolysis. The line drawing shows the CUG^{499} precursor. P1 and P2 denote cleavage sites 1 and 2 (downwards-pointing arrows) respectively. Cleavage at P1 yields VEGF and the 28 kDa N-terminal fragment. Subsequent cleavage at P2, N-terminal to the *Nar*I tag, could yield the 22 and 10 kDa N-terminal fragments, which probably span the N-terminus and C-terminus respectively of the 28 kDa N-terminal fragment. The exact location of site 2 was not determined. The positions of molecular mass markers are indicated (in kDa) at the left in (**B**) and (**C**).

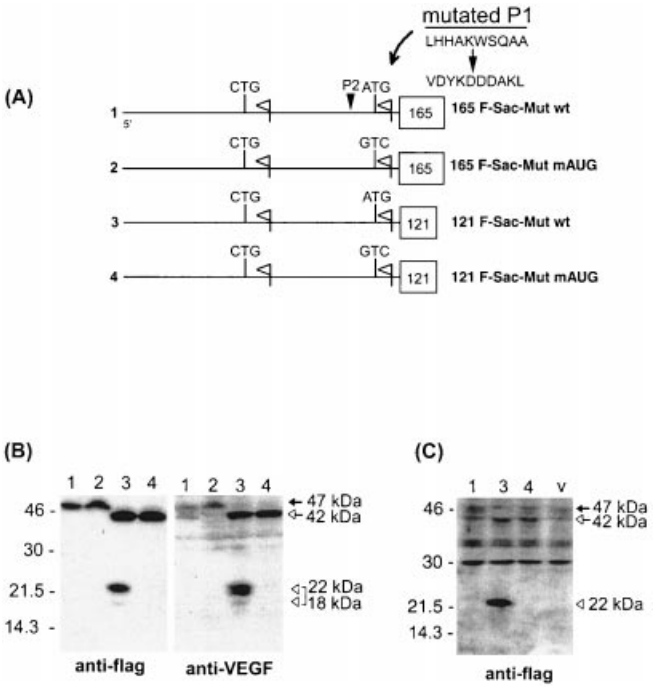

Figure 3 The 47 kDa form is predominant in VEGF$_{165}$

(**A**) Line drawing showing constructs F-Sac-Mut having the *Sac*II tag and mutation/tagging of proteolytic site 1 (P1). The location of proteolytic site 2 (P2) is indicated. (**B**, **C**) COS1 (**B**) and OVCAR3 (**C**) cell lines were transfected with F-Sac-Mut constructs; Western blots of cell lysate were probed under reducing conditions with anti-FLAG and/or anti-VEGF antibodies, as indicated. The positions of molecular mass markers are indicated (in kDa) at the left in (**B**) and (**C**).

cells, the Western blot was probed with anti-FLAG antibody under reducing conditions. Bands of 42 or 47 kDa were seen when CUG^{499} was intact in VEGF$_{121}$ and VEGF$_{165}$ respectively (Figure 2B, lanes 1, 3, 5, 7 and 8). However, when CTG^{499} was mutated (Figure 2B, lanes 2, 4 and 6), the intensities of these bands were decreased, indicating that the 42 and 47 kDa bands were predominantly CUG^{499} products. Additional bands of 22 and 28 kDa (Figure 2B, lanes 1, 3, 5 and 7) and 10 and 28 kDa (lane 8) respectively were detected. The 10, 22 and 28 kDa fragments were probably proteolytic products of the 42/47 kDa precursor forms, which was consistent with the data in Figure 1(C).

Although the 42, 47, 28, 22 and 10 kDa bands were predominantly cell-associated, only the 22 and 47 kDa bands could be detected in CM (Figure 2B, lane 7). When analysed under non-reducing conditions, there was little change in the apparent molecular mass of the 10, 22 and 28 kDa bands, indicating that these proteins were predominantly monomers (results not shown).

When probed with anti-VEGF antibody (Figure 2C), 15/18 and 21/23 kDa bands were present in VEGF$_{121}$ and VEGF$_{165}$ cDNA species respectively. In 121 F-Sac mAUG and 165 F-Sac mAUG (Figure 2C, lanes 1 and 5), the VEGF forms were likely to arise from proteolysis of the precursor proteins rather than from the AUG^{1039} product.

As summarized in Figure 2(D), the VEGF precursor was probably processed at two sites, P1 and P2, to yield VEGF and 10, 22 and 28 kDa N-terminal fragments.

Predominant form of VEGF$_{165}$ is the 47 kDa precursor

Because VEGF could arise by cleavage at site 1 in both CUG^{499} and AUG^{1039} products, this hampered the evaluation of the relative strengths of CUG^{499} and AUG^{1039}. To overcome this difficulty, proteolytic site 1 was mutated by replacing residues 198–207 of the signal peptide in the precursor with FLAG (Figure 3A). Only the C-core in the signal peptide was altered by this mutation. In this experiment, AUG^{1039} proteins had an additional uncleaved 26 residues at the N-terminus and were expected to migrate to a point corresponding to 3.3 kDa larger

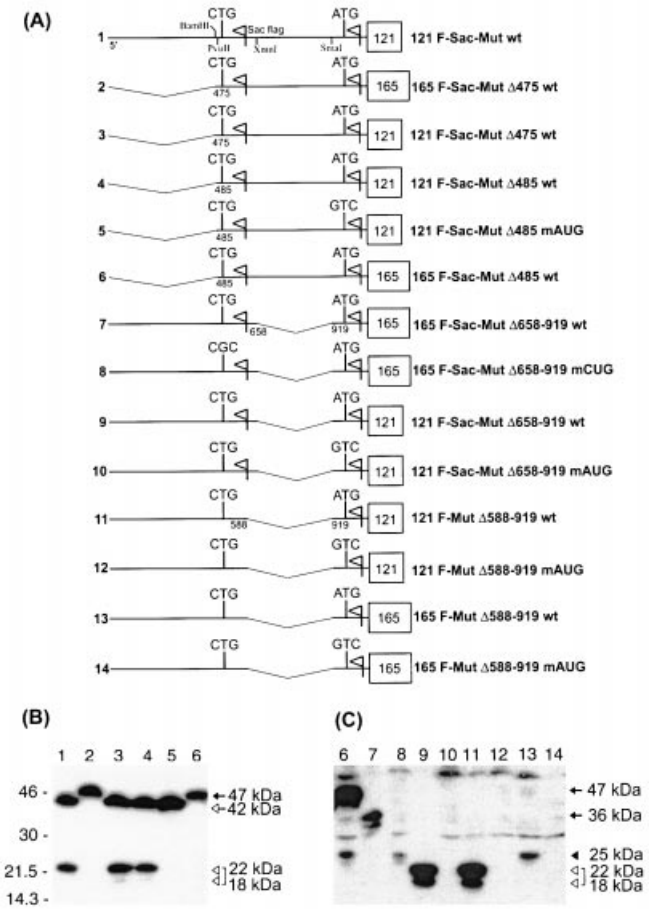

Figure 4 CUG^{499} recognition is enhanced by downstream sequences

(**A**) Line drawing of a full-length VEGF$_{121}$ F-Sac-Mut cDNA and 5′-deletion constructs. Sites *Bam*HI, *Pvu*II, *Sac*II, *Xmn*I and *Sma*I were used for the creation of deletion constructs lacking the first 475 and 485 nt of the 5′ UTR (F-Sac-Mut Δ475 and Δ485 respectively) and of internal deletions of nt 588–919 (F-Mut Δ588–919) and nt 658–919 (F-Sac-Mut Δ658–919). These constructs were transfected into COS1 cells and Western blotting of cell lysates was performed with anti-FLAG antibody under reducing conditions. (**B**, **C**) Lanes 1–6 (**B**) and lanes 6–14 (**C**) of a longer exposure of the blot. The positions of molecular mass markers are indicated (in kDa) at the left of (**B**).

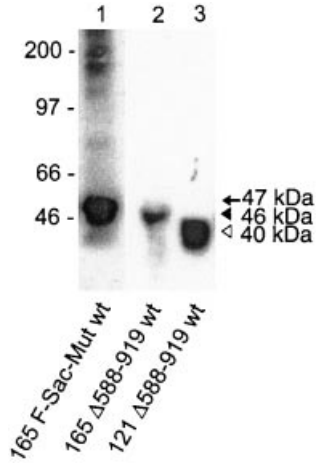

Figure 5 VEGF precursor forms predominantly monomers

Western blot of cell lysate from 165 F-Sac-Mut wt, 165 Δ588–919 wt and 121 Δ588–919 wt, which produced VEGF$_{165}$ precursor and AUG^{1039} forms of VEGF$_{121}$ and VEGF$_{165}$ respectively, probed with the anti-FLAG antibody under non-reducing conditions. The positions of molecular mass markers are indicated (in kDa) at the left.

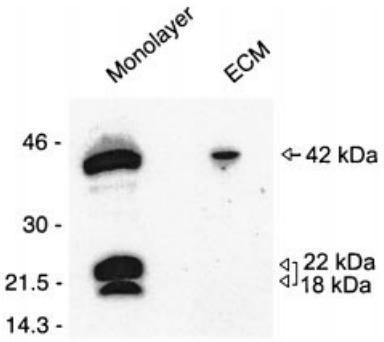

Figure 6 VEGF precursor is detected in the ECM preparation

Western blot of cell monolayer and ECM fractionated from one plate of COS1 cells transfected with 121 F-Sac-Mut wt, probed with the anti-FLAG antibody under reducing conditions. The 18/22 kDa AUG^{1039} form of VEGF$_{121}$ is the positive and negative control respectively in cell monolayer and ECM [15]. The positions of molecular mass markers are indicated (in kDa) at the left.

than mature VEGF, namely 18.3/21.3 kDa for VEGF$_{121}$ and 24.3/26.3 kDa for VEGF$_{165}$ in this experiment, compared with 15/18 and 21/23 kDa in Figure 2(C). The *Sac*II tag permitted the detection of the 22 kDa N-terminal fragment that could arise if processing occurred independently at site 2.

After transfection into COS1 cells, Western blots were probed with the anti-FLAG and anti-VEGF antibodies. In VEGF$_{165}$ the predominant band was the 47 kDa precursor (Figure 3B, lanes 1 and 2). However, 121 F-Sac-Mut wt gave 42 and 18/22 kDa bands (Figure 3B, lane 3), corresponding to the sizes of the precursor and AUG^{1039} forms of VEGF$_{121}$ respectively.

Although constructs 121 and 165 F-Sac-Mut mAUG carried mutations of proteolytic site 1 and GTC$_{1039}$ instead of ATG, processing at site 2 alone might still have occurred in the precursor to yield the 22 kDa N-terminal fragment. This proteolytic product could be detected by anti-FLAG antibody but not by anti-VEGF antibody. However, when probed with the former, constructs 121 and 165 F-Sac-Mut mAUG produced the unprocessed precursors (Figure 3B, lanes 2 and 4), suggesting that processing at site 2 was inefficient when site 1 was mutated.

To examine whether the results above were cell-specific, we conducted a similar experiment in the ovarian cancer cell line OVCAR3 (Figure 3C). When probed with anti-FLAG antibody, the 47 kDa (Figure 3C, lane 1) and 42 kDa (lanes 3 and 4) bands were detected above the background. Construct 121 F-Sac-Mut wt also gave the 18/22 kDa AUG^{1039} form of VEGF$_{121}$ (Figure 3C, lane 2), which is consistent with the results for COS cells.

CUG^{499} recognition in VEGF$_{121}$ and VEGF$_{165}$ is influenced by downstream sequences

CUG^{499} is suboptimal as it lacks the favourable A^{-3} and G^{+4}. To determine whether CUG^{499} recognition is influenced by *cis*-acting element(s), we made 5′ UTR deletions (Figure 4A).

After transfection into COS1 cells, the derived Western blot was analysed with anti-FLAG antibody. CUG^{499} initiation was

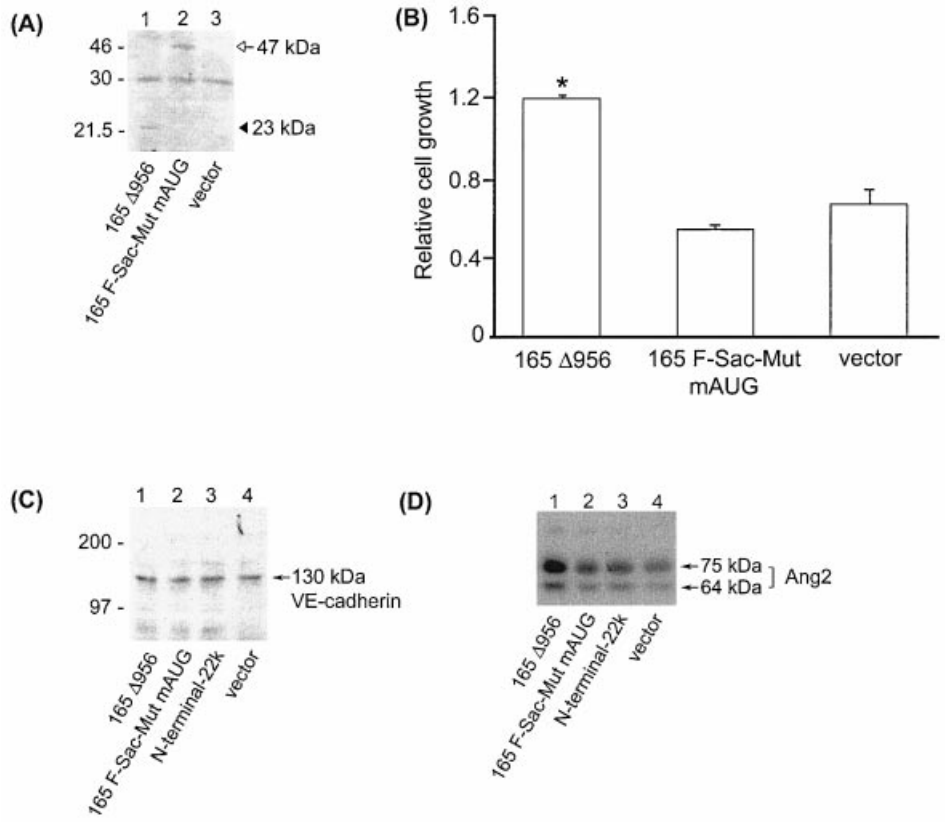

Figure 7 Biological significance of VEGF precursor

(**A**) HUVEC were transfected with 165 Δ956 and 165 F-Sac-Mut mAUG, which produce the bioactive and the CUG^{499} forms of $VEGF_{165}$ respectively. The former construct is similar to that used in a cell proliferation assay [2]. The Western blot of cell lysates was probed with anti-VEGF antibody under reducing conditions. The 30 kDa band might be non-specific because it was also present in the vector lane. (**B**) Cell proliferation assay was performed in triplicate with a Celltiter 96 aqueous one-solution cell proliferation assay (Promega, Madison, WI, U.S.A.) from three separate experiments. Results show D_{490} values and are means ± S.E.M. The Scheffe test was used for statistical analysis. (**C**, **D**) HUVEC were transfected with the above constructs and N-terminal-22k. The Western blots of cell lysates were probed under reducing conditions with antibodies against VE-cadherin (**C**), an endothelium-specific adhesion protein [27,28], and Ang2 (**D**). The 75 and 64 kDa bands correspond to the sizes of glycosylated and non-glycosylated Ang2 respectively [29]. The positions of molecular mass markers are indicated (in kDa) at the left in (**A**) and (**C**).

apparently unaffected despite the removal of 485 nt of the 5′ UTR in $VEGF_{121}$ and $VEGF_{165}$ (Figure 4B, lanes 4 and 6).

To determine whether CUG^{499} initiation was influenced by downstream sequences, two internal deletions were made of nt 658–919 (Δ658–919) and 588–919 (Δ588–919), corresponding to residues 54–140 and 30–140 respectively. In these deletions, the precursors were predicted to be 26 and 29 kDa for $VEGF_{121}$ and 30 and 33 kDa for $VEGF_{165}$ respectively.

The truncated CUG^{499} precursor in 165 F-Sac-Mut Δ658–919 wt produced a 36 kDa band (Figure 4C, lane 7) that was absent when CTG^{499} was mutated (lane 8) and also from the deletion Δ588–919 (lanes 13 and 14). However, CUG^{499} product was not detected in deletions Δ588–919 and Δ658–919 of $VEGF_{121}$ (Figure 4C, lanes 9–12). Both deletions Δ658–919 and Δ588–919 yielded the 18/22 kDa (Figure 4C, lanes 9 and 11) and 25 kDa (lanes 8 and 13) bands, corresponding to the sizes of the AUG^{1039} products of $VEGF_{121}$ and $VEGF_{165}$ respectively.

VEGF precursor yields predominantly monomers

The dimerization of VEGF is essential for biological activity and occurs via disulphide bonds [16]. $VEGF_{165}$ precursor could also form dimers because it has 18 cysteine residues, two of which are at positions 61 and 126 in the N-terminal region. When analysed by Western blotting with the anti-FLAG antibody, the $VEGF_{165}$ precursor and the AUG^{1039} forms of $VEGF_{121}$ and $VEGF_{165}$ migrated at 47, 46 and 40 kDa respectively under non-reducing conditions (Figure 5).

VEGF precursor is associated with the ECM

Although the VEGF precursor was detected in the CM (Figure 2B), a significant portion was cell-associated. To determine whether the latter was associated in part with the ECM, COS1 cells were transfected with 121 F-Sac-Mut wt, containing a mutation of proteolytic site 1 and producing the $VEGF_{121}$ 42 kDa precursor and the 18/22 kDa AUG^{1039} form. Fractionated cell monolayer and ECM were probed with the anti-FLAG antibody.

Previously, $VEGF_{121}$ derived presumably from the AUG^{1039} product was detected in cell monolayers but not in the ECM [15]. In the present study, the 18/22 kDa AUG^{1039} form of $VEGF_{121}$ was also detected only in cell monolayers (Figure 6). The 42 kDa precursor was detected in both cell monolayers and ECM. Even though the protein content of cell monolayers loaded on the gel was 50-fold that of the ECM, the level of the 42 kDa precursor in cell monolayers was 8-fold that in the ECM. Thus a substantial portion of the precursor was likely to be associated with the ECM.

Biological significance of $VEGF_{165}$ precursor

Secreted VEGF can induce the proliferation of endothelial cells such as HUVEC. The VEGF precursor is detectable in CM and might also function as a mitogen. Therefore 165 Δ956 and F-Sac-Mut mAUG, which produced $VEGF_{165}$ and the unprocessed $VEGF_{165}$ precursor respectively, were transfected into HUVEC (Figure 7A). The former construct was the positive control because it was expected to secrete bioactive $VEGF_{165}$. Construct 165 Δ956 induced HUVEC proliferation 2-fold but 165 F-Sac-Mut mAUG did not (Figure 7B).

During tumour angiogenic induction, Ang2 can act co-operatively with VEGF [17]. As Ang2 protein synthesis can also be induced by VEGF in bovine retinal endothelial cells [18], we sought to determine whether the $VEGF_{165}$ precursor acted similarly. HUVEC were transfected with the constructs above and with a new construct, N-terminal-22k, which yielded a product analogous to the 22 kDa N-terminal fragment. After transfection, cell lysates were probed with VE-cadherin and Ang2 antibodies. Although the levels of VE-cadherin were comparable (Figure 7C), the Ang2 level increased 2.5-fold when HUVEC were transfected with construct 165 Δ956, compared with 165 F-Sac-Mut mAUG and N-terminal-22k (Figure 7D).

DISCUSSION

Here we have identified a new VEGF precursor expressed in human ovarian tumours and some fetal tissues. Our studies demonstrate that the precursor undergoes proteolysis at two sites to yield VEGF isoforms and 10, 22 and 28 kDa N-terminal fragments (Figure 8).

Although IRES B (nt 91–483 [10]) could potentially promote initiation from the suboptimal CUG^{499}, this IRES might have little influence under normal conditions. Instead, CUG^{499} recognition could be controlled by at least two separate, overlapping, downstream regions in $VEGF_{121}$ and $VEGF_{165}$. As predicted by the RNAStructure 3.5 program [19], when exon 7 is present, the 72% GC-rich 70 nt region (nt 588–658) could form a specific downstream secondary structure in $VEGF_{165}$ (results not shown). This could slow ribosome scanning, enhancing CUG^{499} recognition. In $VEGF_{121}$, CUG^{499} recognition is influenced by sequences from nt 588 to 919, which contains IRES A (nt 745–1038), predicted to base-pair extensively [9,10]. Thus in $VEGF_{121}$, IRES A might have a dual function in aiding CUG^{499} recognition via the formation of secondary structure and facilitating AUG^{1039} initiation without scanning.

AUG^{1039} initiation could also be controlled in a sequence-specific manner in $VEGF_{121}$ and $VEGF_{165}$. Domains D1–D3 (nt 845–938) in IRES A are predicted to form a Y-shaped secondary structure common to IRES elements [9]. Analysis with the RNAStructure 3.5 program [19] revealed the Y-shaped structure upstream of AUG^{1039} in $VEGF_{121}$ (results not shown); however, the integrity of the IRES A Y-shaped structure is altered and not evident in a similar analysis of $VEGF_{165}$. This is consistent with the role of IRES A in stimulating AUG^{1039} initiation in $VEGF_{121}$ but not in $VEGF_{165}$.

Our results (Figure 2) showed that the precursor and mature products were present at lower intensities when CUG^{499} and AUG^{1039} were mutated. Further, we have found that $VEGF_{121}$ and $VEGF_{165}$ were still produced when the first 588 nt of the 5′ UTR were deleted in mutant AUG constructs, Δ588 mAUG (results not shown) but not in Δ694 mAUG, which lacked the first 694 nt of the 5′ UTR. Because CUG^{499} is preceded by an in-frame UGA^{487} stop codon, the results suggest that one or more initiation codon(s) lies between CUG^{499} and nt 694. Initiations from codons ACG and GUG occur with an efficiency 2.5–5-fold lower than that from CUG [20]. Although CUG^{499} and AUG^{1039} are the predominant initiation codons in VEGF, it is possible that ACG^{502}, GUG^{568} and CUG^{652} might also be used for initiation to yield precursors 1, 23 and 51 residues smaller than that of CUG^{499}. However, judging by the weak intensities of bands from the double-mutant construct in Figure 2, initiations from ACG^{502}, GUG^{568} and CUG^{652} might occur at lower efficiencies.

We confirmed that cleavage at site 1 occurs in the 26-residue signal sequence in the middle portion of the precursor. As predicted with the SignalP-NN and SignalP-HMM programs [21], an N-terminal signal sequence could be present in the precursor between residues 46–67, with low probabilities of

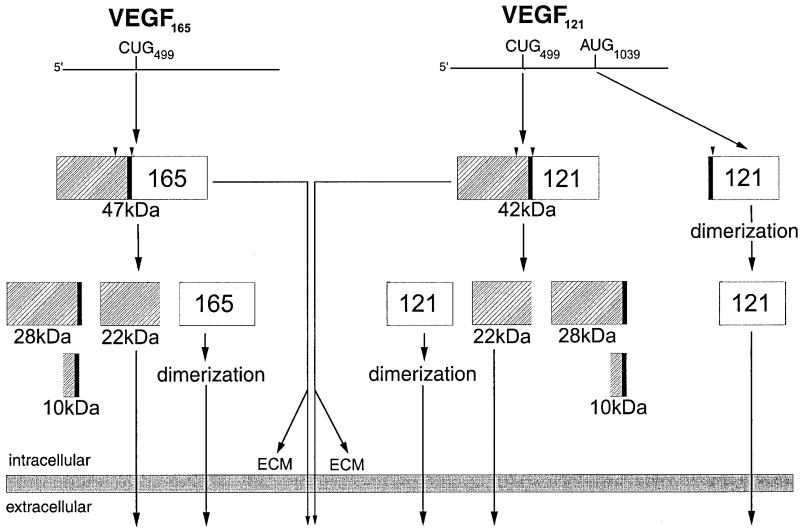

Figure 8 Schematic representation of the synthesis and processing of VEGF precursors

Arrows lead from CUG^{499} initiation to the proteolysis of precursors and secretion of the precursors, $VEGF_{121}$ and $VEGF_{165}$ and the 22 kDa N-terminal fragment, and from AUG^{1039} initiation to the dimerization and secretion of $VEGF_{121}$. Arrowheads indicate proteolytic sites.

cleavage between Ala^{67} and Val^{68}. The predicted product from this cleavage is an 8 kDa N-terminal fragment detectable in construct F-Sac, because it contains the FLAG tag. However, the predominant bands found were 22 and 28 kDa, indicating that cleavage did not occur between Ala^{67} and Val^{68}.

Previous studies have shown that members of the platelet-derived growth factor (PDGF)/VEGF family, including PDGF-AA, VEGF-C and VEGF-D, are synthesized as precursors that undergo proteolysis [22–24]. Alignment of PDGF-AA and VEGF precursor sequences (using the MegAlign Program; results not shown) showed similarity between the PDGF-AA proteolytic site (i.e. KRSIEE; single-letter amino acid codes) and those predicted for site 2 in the VEGF precursor (RRGAEE). A similar analysis showed similarity between the intracellular cleavage site in the VEGF-C precursor (i.e. RRSLPA) and the VEGF proteolytic site 1 (KWSQAA). Both cleavages yield the bioactive VEGF and VEGF-C, suggesting that both precursors might be processed by similar protease(s). Thus precursor synthesis and proteolysis might be evolutionarily conserved in the PDGF/VEGF family and might be important in regulating angiogenesis.

We have found that VEGF expression is greatest in tissues known to undergo active angiogenesis (i.e. ovarian tumours, placenta, and fetal ovary, heart, lung and spleen) [25,26]. The high levels of VEGF in these tissues probably originate from the processing of both CUG^{499} and AUG^{1039} products. Processing of CUG^{499}-derived precursors might be a major source for active VEGF products that mediate angiogenesis in ovarian tumours and some fetal tissues.

In summary, we have identified a new VEGF precursor expressed in ovarian tumours and some fetal tissues, and have shown that, unlike VEGF, the precursor interacts with the ECM. The VEGF precursor is inactive in stimulating HUVEC proliferation and Ang2 production, suggesting that it might function as a storage form that can be processed into active VEGF isoforms in either the cell or ECM.

We thank Jean-Louis Vigne for his help and discussion during the early phase of this project, and Dale Leitman, Patty Culp, Yu-Long Hu, Pedro Aza-Blanc and Tom Kornberg for useful advice and discussion. This study was supported in part by grant PO1-CA 64602 from the National Cancer Institute.

REFERENCES

1 Ferrara, N. (1999) Molecular and biological properties of vascular endothelial growth factor. J. Mol. Med. **77**, 527–543
2 Houck, K. A., Ferrara, N., Winer, J., Cachianes, G., Li, B. and Leung, D. W. (1991) The vascular endothelial growth factor family: identification of a fourth molecular species and characterization of alternative splicing of RNA. Mol. Endocrinol. **5**, 1806–1814
3 Tischer, E., Mitchell, R., Hartman, T., Silva, M., Gospodarowicz, D., Fiddes, J. C. and Abraham, J. A. (1991) The human gene for vascular endothelial growth factor. Multiple protein forms are encoded through alternative exon splicing. J. Biol. Chem. **266**, 11947–11954
4 Ferrara, N. and Henzel, W. J. (1989) Pituitary follicular cells secrete a novel heparin-binding growth factor specific for vascular endothelial cells. Biochem. Biophys. Res. Commun. **161**, 851–858
5 Carmeliet, P., Ng, Y. S., Nuyens, D., Theilmeier, G., Brusselmans, K., Cornelissen, I., Ehler, E., Kakkar, V. V., Stalmans, I., Mattot, V. et al. (1999) Impaired myocardial angiogenesis and ischemic cardiomyopathy in mice lacking the vascular endothelial growth factor isoforms $VEGF_{164}$ and $VEGF_{188}$. Nat. Med. (N.Y.) **5**, 495–502
6 Keck, P. J., Hauser, S. D., Krivi, G., Sanzo, K., Warren, T., Feder, J. and Connolly, D. T. (1989) Vascular permeability factor, an endothelial cell mitogen related to PDGF. Science **246**, 1309–1312
7 Leung, D. W., Cachianes, G., Kuang, W. J., Goeddel, D. V. and Ferrara, N. (1989) Vascular endothelial growth factor is a secreted angiogenic mitogen. Science **246**, 1306–1309
8 Kozak, M. (1999) Initiation of translation in prokaryotes and eukaryotes. Gene **234**, 187–208
9 Akiri, G., Nahari, D., Finkelstein, Y., Le, S. Y., Elroy-Stein, O. and Levi, B. Z. (1998) Regulation of vascular endothelial growth factor (VEGF) expression is mediated by internal initiation of translation and alternative initiation of transcription. Oncogene **17**, 227–236
10 Huez, I., Creancier, L., Audigier, S., Gensac, M. C., Prats, A. C. and Prats, H. (1998) Two independent internal ribosome entry sites are involved in translation initiation of vascular endothelial growth factor mRNA. Mol. Cell. Biol. **18**, 6178–6190
11 Miller, D. L., Dibbens, J. A., Damert, A., Risau, W., Vadas, M. A. and Goodall, G. J. (1998) The vascular endothelial growth factor mRNA contains an internal ribosome entry site. FEBS Lett. **434**, 417–420
12 Stein, I., Itin, A., Einat, P., Skaliter, R., Grossman, Z. and Keshet, E. (1998) Translation of vascular endothelial growth factor mRNA by internal ribosome entry: implications for translation under hypoxia. Mol. Cell. Biol. **18**, 3112–3119
13 Levy, A. P., Levy, N. S., Wegner, S. and Goldberg, M. A. (1995) Transcriptional regulation of the rat vascular endothelial growth factor gene by hypoxia. J. Biol. Chem. **270**, 13333–13340
14 Shima, D. T., Kuroki, M., Deutsch, U., Ng, Y. S., Adamis, A. P. and D'Amore, P. A. (1996) The mouse gene for vascular endothelial growth factor. Genomic structure, definition of the transcriptional unit, and characterization of transcriptional and post-transcriptional regulatory sequences. J. Biol. Chem. **270**, 3877–3883
15 Park, J. E., Keller, G. A. and Ferrara, N. (1993) The vascular endothelial growth factor (VEGF) isoforms: differential deposition into the subepithelial extracellular matrix and bioactivity of extracellular matrix-bound VEGF. Mol. Biol. Cell **4**, 1317–1326
16 Potgens, A. J., Lubsen, N. H., van Altena, M. C., Vermeulen, R., Bakker, A., Schoenmakers, J. G., Ruiter, D. J. and de Waal, R. M. (1994) Covalent dimerization of vascular permeability factor/vascular endothelial growth factor is essential for its biological activity. Evidence from Cys to Ser mutations. J. Biol. Chem. **26**, 32879–32885
17 Holash, J., Maisonpierre, P. C., Compton, D., Boland, P., Alexander, C. R., Zagzag, D., Yancopoulos, G. D. and Wiegand, S. J. (1999) Vessel cooption, regression, and growth in tumors mediated by angiopoietins and VEGF. Science **284**, 1994–1998
18 Oh, H., Takagi, H., Suzuma, K., Otani, A., Matsumura, M. and Honda, Y. (1999) Hypoxia and vascular endothelial growth factor selectively up-regulate angiopoietin-2 in bovine microvascular endothelial cells. J. Biol. Chem. **274**, 15732–15739
19 Mathews, D. H., Sabina, J., Zuker, M. and Turner, D. H. (1999) Expanded sequence dependence of thermodynamic parameters improves prediction of RNA secondary structure. J. Mol. Biol. **288**, 911–940
20 Mehdi, H., Ono, E. and Gupta, K. C. (1990) Initiation of translation at CUG, GUG, and ACG codons in mammalian cells. Gene **91**, 173–178
21 Nielsen, H., Engelbrecht, J., Brunak, S. and von Heijne, G. (1997) Identification of prokaryotic and eukaryotic signal peptides and prediction of their cleavage sites. Protein Eng. **10**, 1–6
22 Östman, A., Thyberg, J., Westermark, B. and Heldin, C. H. (1992) PDGF-AA and PDGF-BB biosynthesis: proprotein processing in the Golgi complex and lysosomal degradation of PDGF-BB retained intracellularly. J. Cell Biol. **118**, 509–519
23 Joukov, V., Sorsa, T., Kumar, V., Jeltsch, M., Claesson-Welsh, L., Cao, Y., Saksela, O., Kalkkinen, N. and Alitalo, K. (1997) Proteolytic processing regulates receptor specificity and activity of VEGF-C. EMBO J. **16**, 3898–3911
24 Stacker, S. A., Stenvers, K., Caesar, C., Vitali, A, Domagala, T., Nice, E., Roufail, S., Simpson, R. J., Moritz, R., Karpanen, T. et al. (1999) Biosynthesis of vascular endothelial growth factor-D involves proteolytic processing which generates non-covalent homodimers. J. Biol. Chem. **274**, 32127–32136
25 Shifren, J. L., Doldi, N., Ferrara, N., Mesiano, S. and Jaffe, R. B. (1994) In the human fetus, vascular endothelial growth factor is expressed in epithelial cells and myocytes, but not vascular endothelium: implications for mode of action. J. Clin. Endocrinol. Metab. **79**, 316–322
26 Gordon, J. D., Mesiano, S., Zaloudek, C. J. and Jaffe, R. B. (1996) Vascular endothelial growth factor localization in human ovary and fallopian tubes: possible role in reproductive function and ovarian cyst formation. J. Clin. Endocrinol. Metab. **81**, 353–359
27 Lewalle, J. M., Bajou, K., Desreux, J., Mareel, M., Dejana, E., Noel, A. and Foidart, J. M. (1997) Alteration of interendothelial adherens junctions following tumor cell–endothelial cell interaction in vitro. Exp. Cell Res. **237**, 347–356
28 Esser, S., Lampugnani, M. G., Corada, M., Dejana, E. and Risau, W. (1998) Vascular endothelial growth factor induces VE-cadherin tyrosine phosphorylation in endothelial cells. J. Cell Sci. **111**, 1853–1865
29 Davis, S., Aldrich, T. H., Jones, P. F., Acheson, A., Compton, D. L., Jain, V., Ryan, T. E., Bruno, J., Radziejewski, C., Maisonpierre, P. C. and Yancopoulos, G. D. (1996) Isolation of angiopoietin-1, a ligand for the TIE2 receptor, by secretion-trap expression cloning. Cell **87**, 1161–1169

Received 14 March 2001/29 May 2001; accepted 24 July 2001